DRAFT VERSION APRIL 2, 2020
Typeset using LATEX **twocolumn** style in AASTeX62

Against the Planetary Interpretation of PTFO 8-8695b

L. G. BOUMA[1] AND J. N. WINN[1]

[1] *Department of Astrophysical Sciences, Princeton University, 4 Ivy Lane, Princeton, NJ 08540, USA*

(Received April 2, 2020; Revised —; Accepted —)

Submitted to AAS journals.

ABSTRACT

PTFO 8-8695b could be the youngest, shortest-period hot Jupiter known. However it has not been shown to be a planet. TESS recently observed PTFO 8-8695 for one month. The TESS light-curve shows that the dominant variability in this system is a sinusoidal modulation with a "long" period P_ℓ of 11.96 hours, likely caused by stellar rotation. Also present is a complex signal, previously identified as the planet candidate, that repeats with a "short" period P_s of 10.74 hours. The "long" and "short" signals show the expected beat every 4.48 days. There is a dip in the complex, short-period signal. However ground-based photometry from the past decade shows that the orbital phase of the dip seems to have instantaneously jumped, at least once, and maybe twice. The TESS epoch of the dip is consistent with recent observations by Tanimoto et al., and differs from the discovery epoch by 5.14 hours. Planets do not "jump" in orbital phase. PTFO 8-8695 therefore seems broadly consistent with the "transient dipping" phenomenology observed in many young M dwarfs, and seems unlikely to be a planet.

1. INTRODUCTION

If it were a planet, PTFO 8-8695b would be exceptional. A transiting hot Jupiter, orbiting a $\approx$3 Myr old M dwarf in ORION would make it the youngest hot Jupiter known. Its orbital period of only 12 HOURS would also make it the shortest period hot Jupiter known.

2. OBSERVATIONS

PTFO 8-8695 was observed by TESS with Camera 1, CCD 1, from December 15, 2018 to January 6, 2019, during the sixth sector of science operations. The star is designated TIC 264461976 in the TESS Input Catalog (Stassun et al. 2018). The pixel data for an 11×11 array surrounding PTFO 8-8695 were averaged into 2-minute stacks by the onboard computer. Each 2048×2048 image was also averaged into 30-minute stacks, and saved as a "full frame image" (FFI).

The data were downlinked via the Deep Space Network[1], and the spacecraft timestamps were calibrated against the ground-station clocks. The spacecraft clock times were then transformed by the Payload Operations Center into the *Temps Dynamique Barycentrique* (TDB) reference system. The images were then reduced to lightcurves by the Science Processing Operations Center (SPOC) at NASA Ames (Jenkins et al. 2016).

We began our analysis with the Presearch Data Conditioning (PDC) lightcurve, which has had non-astrophysical variability removed through the methods discussed by Smith et al. (2017a) and Smith et al. (2017b). We then processed the lightcurve as follows. First, we removed all points with non-zero quality flags. This removed data that might have been adversely affected by "momentum dumps," the firing of thrusters and resetting of reaction wheels[2] that took place every 2.5 days during sector 2. The data during these events were assigned quality flags corresponding to "Reaction Wheel Desaturation Event" and "Manual Exclude" (Tenenbaum & Jenkins 2018, Table 28). For WASP-4, these flags were simultaneously set for 54 distinct cadences, and there were 10 momentum dumps, averaging about 10 minutes of flagged data per dump. Out of caution, we clipped out an additional 10 minutes before and after every momentum dump. We also removed the data within the first and last hours of both orbits, because of correlated red noise that appears during those time ranges.

All told, we removed 8% of the original data points, and were left with 18,165 measurements of the relative flux of WASP-4. We normalized the data by dividing out the median flux. We converted the timestamps from $\mathrm{BTJD_{TDB}}$ into $\mathrm{BJD_{TDB}}$ by adding the appropriate 2,457,000 day offset (Tenenbaum & Jenkins 2018). Many of these and subsequent processing steps were performed using `astrobase` (Bhatti et al. 2018). We did not "flatten" the lightcurves, as is often done with splines, polynomials, or Gaussian processes.

Corresponding author: L. G. Bouma
luke@astro.princeton.edu

[1] deepspace.jpl.nasa.gov

[2] The spacecraft pointing and momentum dumps are described in the data release notes: archive.stsci.edu/missions/tess/doc/tess_drn/tess_sector_07_drn09_v03.pdf

Instead, we modeled the out-of-transit flux variations simultaneously with the transit parameters, as described below.

3. ANALYSIS

3.1. *Visual Inspection*

Our initial inspection of the light-curve, in both its 2-minute PDCSAP and 30-minute FFI forms, revealed an obvious beat signal (Figure 1, top panel).

As a precursor to more detailed analysis, we calculated generalized Lomb-Scargle periodograms using `astrobase` (Lomb 1976; Scargle 1982; VanderPlas & Ivezić 2015; Bhatti et al. 2018). The two largest peaks in the Lomb-Scargle periodogram of the light-curve were clearly separated at $P_s \approx 0.448$ days and $P_\ell \approx 0.499$ days. The P_ℓ peak had the larger amplitude of the two. Smaller harmonics from each of these dominant two signals were also present.

Initial fitting experiments with splines showed that subtracting out the long-period signal, the short-period signal dominated the periodogram, and vice-versa. However it quickly became clear that a mroe careful modelling approach than "flattening" the light-curve with splines or Gaussian proceses would be preferable, in order to preserve the power at each frequency.

3.2. *Model Fitting*

We opted to model the light-curve as a linear combination of Fourier harmonics at the short and long periods, plus a transit at the short period. Symbolically,

$$f = f_s + f_\ell = f_{\rm transit,s} + f_{\rm Fourier,s} + f_{\rm Fourier,\ell}, \tag{1}$$

where f_s is the relative flux at the short period, and f_ℓ is the flux at the long period. Decomposing each term,

$$\begin{aligned} f =& f_{\rm transit,s} + \sum_{n=1}^{n=N} A_n \sin(n\omega_s t) + \sum_{n=1}^{n=N} B_n \cos(n\omega_s t) \\ &+ \sum_{m=1}^{m=M} A_m \sin(m[\omega_\ell t + \phi_\ell]) + \sum_{m=1}^{m=M} B_m \cos([m\omega_\ell t + \phi_\ell]), \end{aligned} \tag{2}$$

for N and M the total number of harmonics at the short and long period, respective, A_i and B_i for each harmonic term, and $\omega_i = 2\pi/P_i$ the angular frequency for i the short or long period index. We fixed the "phase-offset" for the short period signal to be zero, and let the reference time of the long period signal float by introducing ϕ_ℓ. Since we did not a priori know how many harmonics would be appropriate, we let the number of harmonics vary, and used the Bayesian information criterion to choose the appropriate model.

For example, one possible model could be a transit, plus $N = 2$ harmonics of sines and cosines at the short period, plus $M = 1$ harmonics at the long period. In this case, the free parameters would be as follows. For the transit, we would fit for the impact parameter, the planet-to-star radius ratio, two quadratic limb darkening parameters, the planet orbital period (equal to the short period), the reference time for the transit, and the mean flux. There would be 4 additional Fourier amplitudes at the short period, plus 2 Fourier amplitudes at the long period, and well as the long period itself and its phase. For this case, we therefore fitted 14 free parameters.

The periodogram of the final residual (Figure 1 bottom row) shows a weakly significant, poorly resolved peak at ≈8 days, consistent with the visual impression in the time domain that there could be a weak long-period signal present.

3.3. *Blend considerations*

The TESS pixels are ≈ 21" per side, and so we need to consider whether light from neighboring stars could affect the photometry. The scene is shown in Figure 3. The pixels used to measure the background level are indicated with an '`X`' hatch, and the pixels used for the final light-curve are shown with the '`/`' hatch.

The target star, PTFO 8-8605 (TIC 264461976), has a T-band magnitude of 14.0, and its position is shown with a star. The other (unlabeled) star inside the target aperture, TIC 264461979, has $T = 16.8$ and so cannot contribute a signal with relative amplitude 10%. The only neighbor that is sufficiently close and bright that its light might contaminate the target star is TIC 264461980, with $T = 14.8$, which we denote "Star A". Star A is 23.6" NW of our target, and based on the magnitude difference could contribute up to 48% the flux of our target star, PTFO 8-8695.

Because PTFO 8-8695 has previously been identified to have periodicity consistent with our measurement of P_s, our main concern regarding blending is the degree to which we can be certain that the long-period signal at P_ℓ also originates from PTFO 8-8695. We took two approaches towards determining the source of the long-period signal.

First, we examined the CDIPS full frame image light-curves of the target, which are available on MAST (Bouma et al. 2019). The maximal peak-to-peak beat amplitude is consistently ≈10% across apertures of radii 1, 1.5, and 2.25 pixels. If Star A were the source of the long-period variability, we would expect the peak variability amplitude to be smallest in the 1 pixel aperture, based on the separation of the sources (Figure 3, bottom). From this test alone, it seems unlikely that Star A is the source of the long-period signal.

Second, we examined the light-curve of each pixel in the scene individually. We opted to use the interactive tools implemented in `lightkurve` (Lightkurve Collaboration et al. 2018). If Star A were the source of the long-period variability, we would expect the pixels nearest to Star A to show a sinusoidal signal with amplitude exceeding 10%. We find no evidence for this being the case. The pixel directly below Star A does not clearly show the sinusoidal variability, and the peak-to-peak variability in that pixel is $\lesssim 8\%$. In contrast, the south-easternmost pixel within PTFO 8-8695's aperture (the pixel furthest from Star A that was used in the optimal aperture) shows the P_ℓ sinusoidal variability signal at ≈ 10% amplitude.

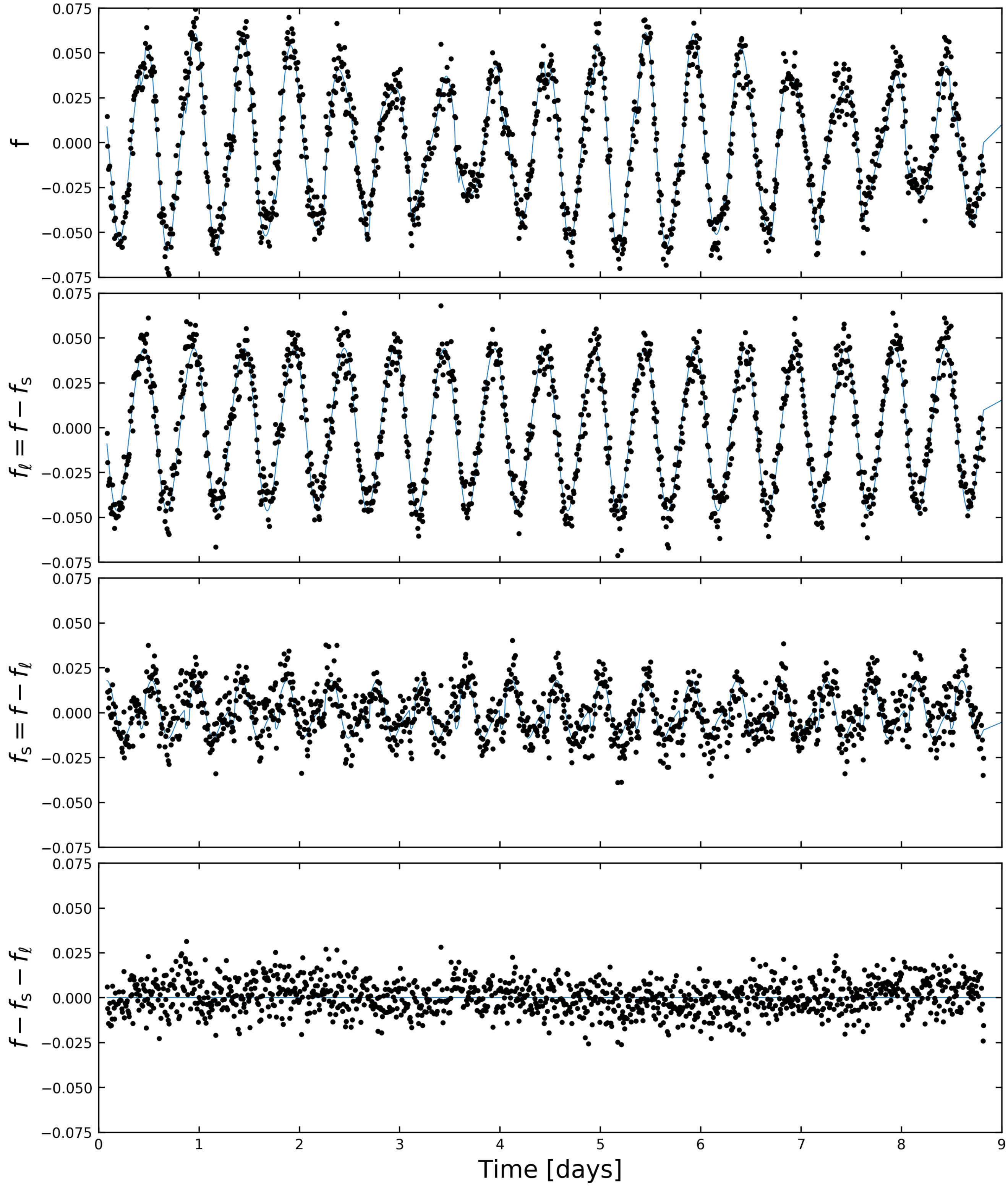

Figure 1. TESS light-curve of PTFO 8-8695 (Sector 6, Orbit 1). *Top*: "Raw" `PDCSAP` mean-subtracted relative flux versus time. The beat period of 4.48 days is visible by eye. The model plotted underneath the data includes 2 harmonics at the long period P_ℓ, plus 2 harmonics and a transit at the short period P_s. *Upper middle*: Long-period signal, equal to the raw signal minus the short-period signal. *Lower middle*: Short-period signal, equal to the raw signal minus the long-period signal. *Bottom*: residual. The data are binned from 2 to 10 minute cadence as a convenience for plotting and fitting.

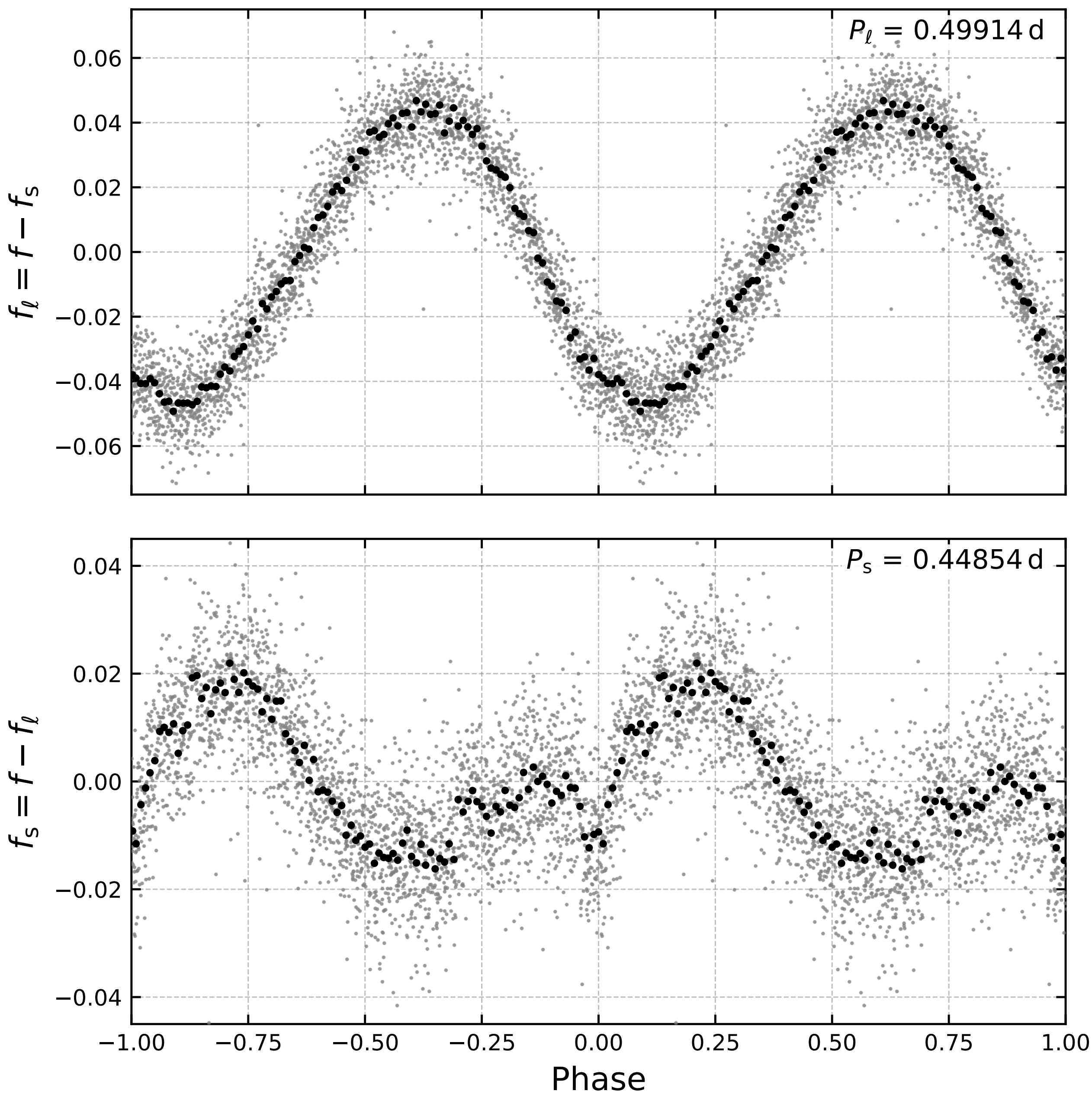

Figure 2. Phase-folded long and short-period signals. *Top*: Long-period signal, as in Figure 1. *Bottom*: Short-period signal. The reference phase is set to the "planetary" dip. Gray points are the 10 minute cadence PDCSAP flux. Black points are binned to 100 points per period.

As there is no evidence in favor of a blend scenario, we conclude that both the P_s and P_ℓ signals originate from PTFO 8-8695.

4. DISCUSSION

The TESS dip does not phase up where it is supposed to...

5. CONCLUSIONS

Software: astrobase (Bhatti et al. 2018), astropy (Astropy Collaboration et al. 2018), astroquery (Ginsburg et al. 2018), corner (Foreman-Mackey 2016), emcee (Foreman-Mackey et al. 2013), IPython (Pérez & Granger 2007), lightkurve (Lightkurve Collaboration et al. 2018), matplotlib (Hunter 2007), MESA (Paxton et al. 2011, 2013, 2015) numpy (Walt et al. 2011), pandas (McKinney 2010), radvel (Fulton et al. 2018), scipy (Jones et al. 2001).

REFERENCES

Astropy Collaboration, Price-Whelan, A. M., Sipőcz, B. M., et al. 2018, AJ, 156, 123

Bhatti, W., Bouma, L. G., & Wallace, J. 2018, astrobase, https://doi.org/10.5281/zenodo.1469822

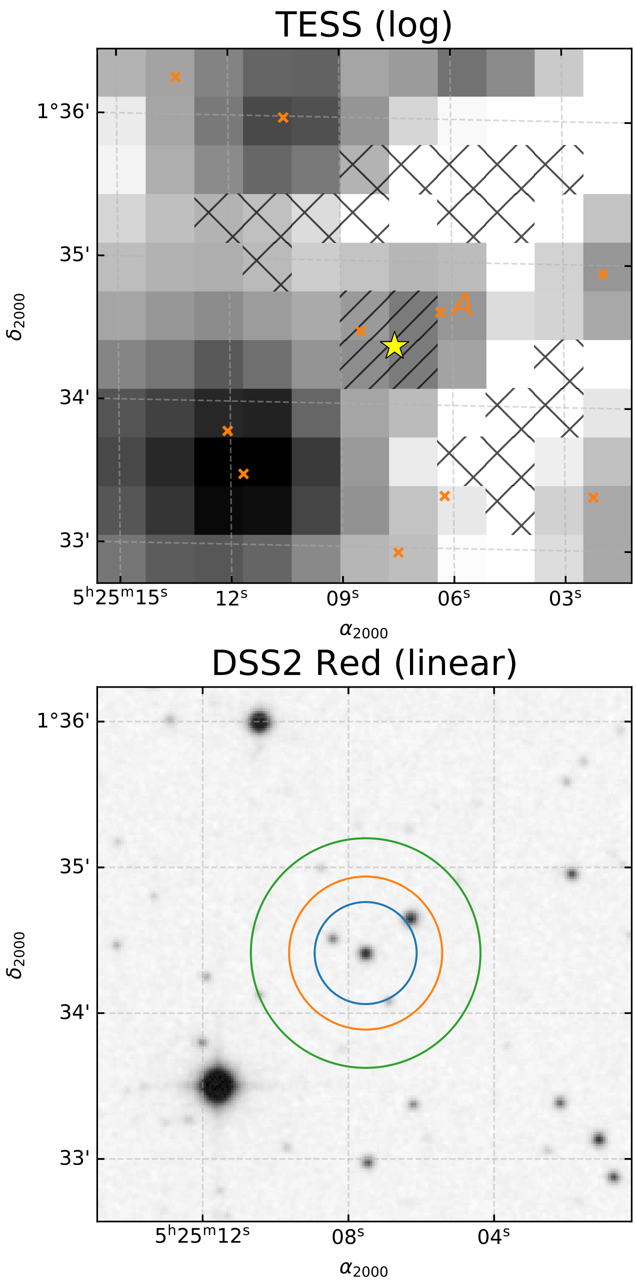

Figure 3. Scene used for blend analysis. *Top:* Mean TESS image of PTFO 8-8695 over Sector 6, with a log-stretch. The position of PTFO 8-8695 is shown with a yellow star. Neighbors with $T < 17$ are shown with orange crosses. The apertures used to measure the background and target star flux are shown with X and / hatches, respectively. *Bottom:* Digitized Sky Survey R-band image of the same field, with a linear stretch. The circles show apertures of radii 1, 1.5, and 2.25 pixels used in part of our blend analysis. The pixel level TESS data show that "Star A" does not contribute variability at either of the two observed periods (see Section 3.3).

Bouma, L. G., Hartman, J. D., Bhatti, W., Winn, J. N., & Bakos, G. Á. 2019, ApJS, 245, 13

Ciardi, D. R., Eyken, J. C. v., Barnes, J. W., et al. 2015, The Astrophysical Journal, 809, 42, publisher: IOP Publishing

Foreman-Mackey, D. 2016, The Journal of Open Source Software, 24

Foreman-Mackey, D., Hogg, D. W., Lang, D., & Goodman, J. 2013, PASP, 125, 306

Fulton, B. J., Petigura, E. A., Blunt, S., & Sinukoff, E. 2018, PASP, 130, 044504

Ginsburg, A., Sipocz, B., Madhura Parikh, et al. 2018, Astropy/Astroquery: V0.3.7 Release

Hunter, J. D. 2007, Computing in Science & Engineering, 9, 90

Jenkins, J. M., Twicken, J. D., McCauliff, S., et al. 2016, Software and Cyberinfrastructure for Astronomy IV, 9913, 99133E

Jones, E., Oliphant, T., Peterson, P., et al. 2001, Open source scientific tools for Python

Lightkurve Collaboration, Cardoso, J. V. d. M., Hedges, C., et al. 2018, Lightkurve: Kepler and TESS time series analysis in Python, Astrophysics Source Code Library, ascl:1812.013

Lomb, N. R. 1976, Astrophysics and Space Science, 39, 447

McKinney, W. 2010, in Proceedings of the 9th Python in Science Conference, ed. S. van der Walt & J. Millman, 51

Onitsuka, M., Fukui, A., Narita, N., et al. 2017, Publications of the Astronomical Society of Japan, 69

Paxton, B., Bildsten, L., Dotter, A., et al. 2011, ApJS, 192, 3

Paxton, B., Cantiello, M., Arras, P., et al. 2013, ApJS, 208, 4

Paxton, B., Marchant, P., Schwab, J., et al. 2015, ApJS, 220, 15

Pérez, F., & Granger, B. E. 2007, Computing in Science and Engineering, 9, 21

Raetz, S., Schmidt, T. O. B., Czesla, S., et al. 2016, Monthly Notices of the Royal Astronomical Society, 460, 2834

Scargle, J. D. 1982, The Astrophysical Journal, 263, 835

Smith, J. C., Morris, R. L., Jenkins, J. M., et al. 2017a, Kepler Science Document, 7

Smith, J. C., Stumpe, M. C., Jenkins, J. M., et al. 2017b, Kepler Science Document, 8

Stassun, K. G., Oelkers, R. J., Pepper, J., et al. 2018, AJ, 156, 102

Tanimoto, Y., Yamashita, T., Ui, T., et al. 2020, PASJ, arXiv:2001.00148 [astro-ph.EP]

Tenenbaum, P., & Jenkins, J. 2018, TESS Science Data Products Description Document, EXP-TESS-ARC-ICD-0014 Rev D, https://archive.stsci.edu/missions/tess/doc/EXP-TESS-ARC-ICD-TM-0014.pdf

van Eyken, J. C., Ciardi, D. R., von Braun, K., et al. 2012, The Astrophysical Journal, 755, 42

VanderPlas, J. T., & Ivezić, Ž. 2015, The Astrophysical Journal, 812, 18

Walt, S. v. d., Colbert, S. C., & Varoquaux, G. 2011, Computing in Science & Engineering, 13, 22

Yu, L., Winn, J. N., Gillon, M., et al. 2015, The Astrophysical Journal, 812, 48

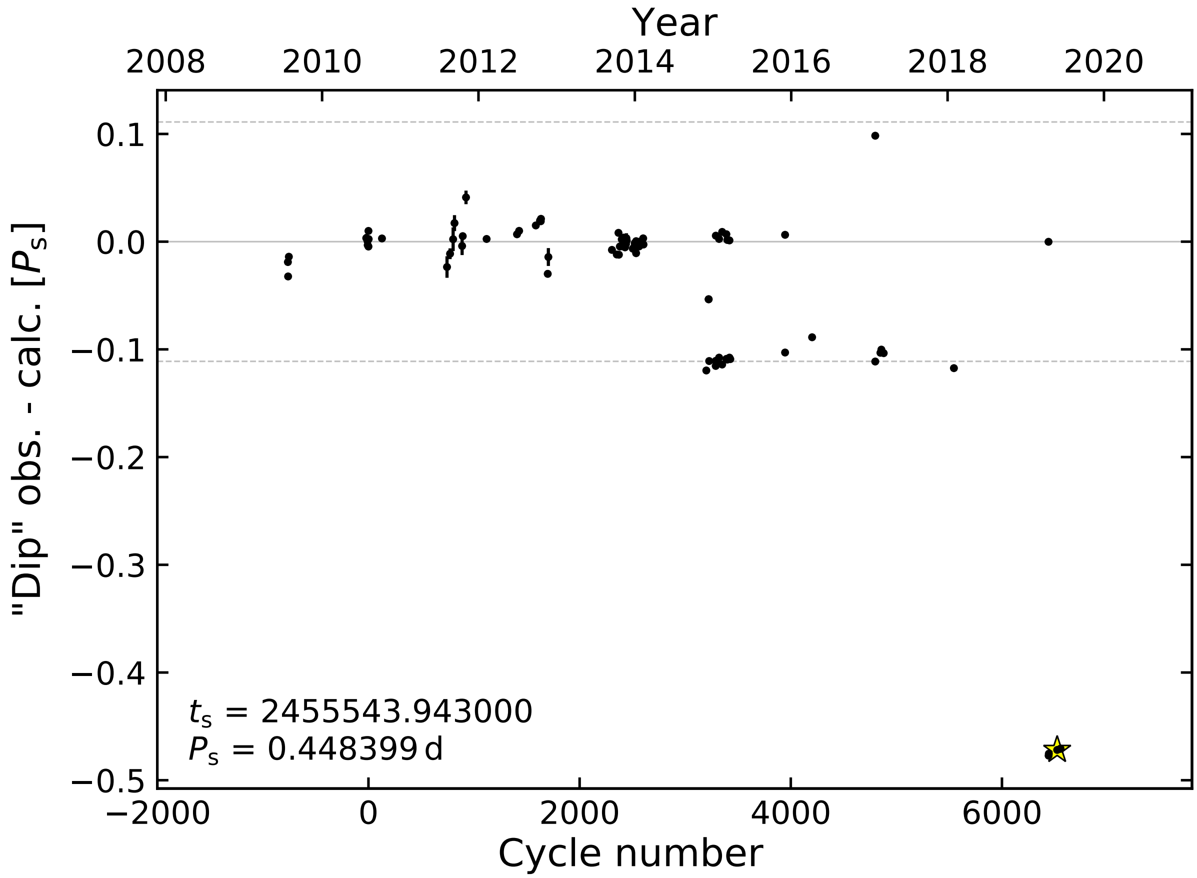

Figure 4. Timing residuals for PTFO 8-8695b from a decade of monitoring. Black points are times of "dips", minus the indicated linear ephemeris. The y-axis is given in units of phase for the short-period signal. The star shows the binned TESS ephemeris. "Dips" have been observed by van Eyken et al. (2012), Ciardi et al. (2015), Yu et al. (2015), Raetz et al. (2016), Onitsuka et al. (2017), and Tanimoto et al. (2020). Certain dips (*e.g.*, the one at phase 0 in mid-2019) are consistent with noise, and were likely reported because something was *expected*, rather than convincingly *observed*. Horizontal dashed lines are drawn at $\pm(P_\ell - P_s)/P_s$, highlighting what could be either a numerical coincidence or an observational bias. The orbital phase observed by TESS is consistent with that of Tanimoto et al. (2020), and quite different from the original phase.

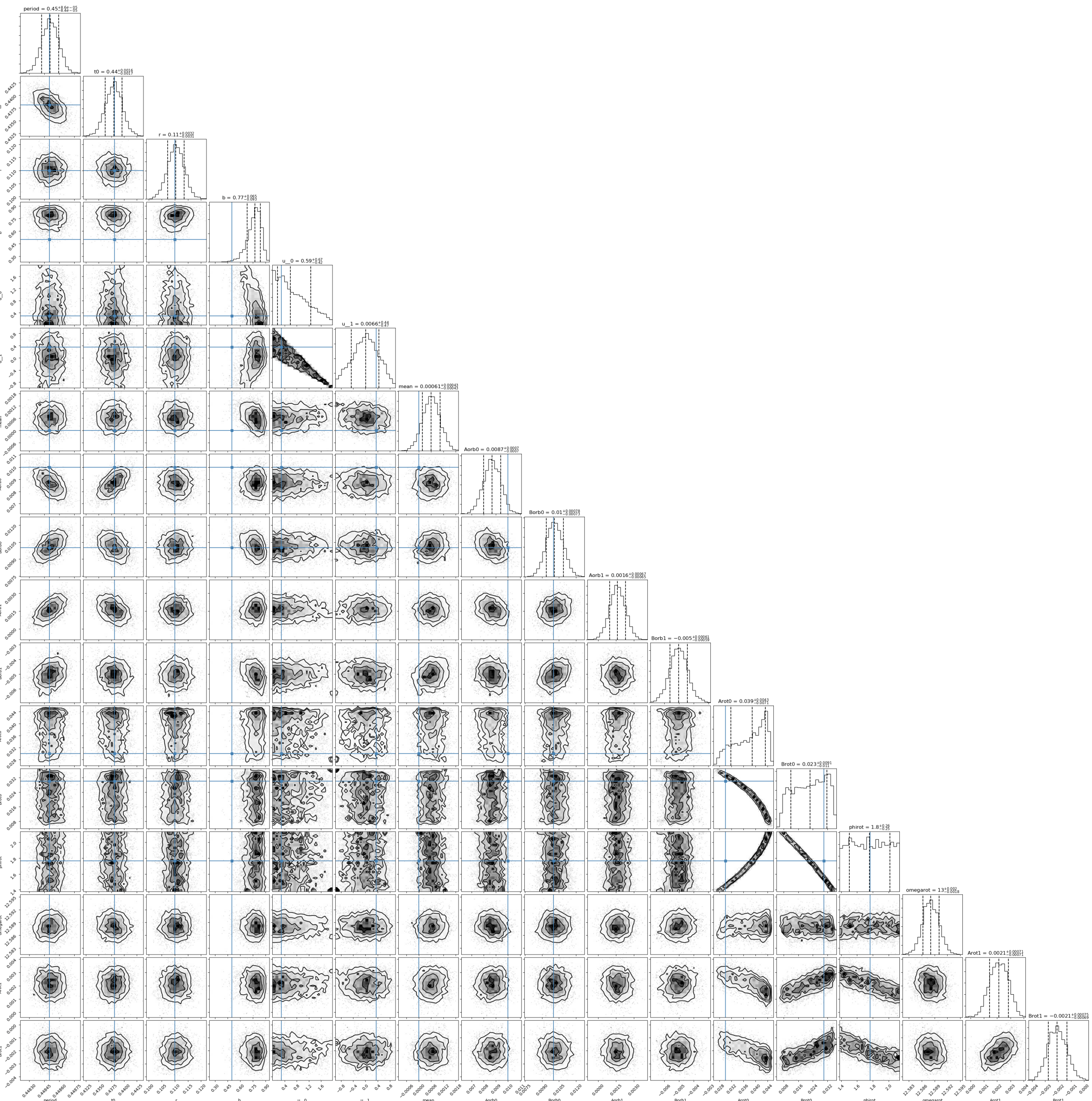

Figure 5. foo. bar